ELSEVIER

Contents lists available at ScienceDirect

# Bioresource Technology

journal homepage: www.elsevier.com/locate/biortech





# One cell-two wells bio-refinery: Demonstrating cyanobacterial chassis for co-production of heterologous and natural hydrocarbons

Kaustubh R. Sawant <sup>a,1</sup>, Aditya P. Sarnaik <sup>a,c,1</sup>, Prashant Savvashe <sup>a,b</sup>, Nima Hajinajaf <sup>c</sup>, Parker Poole <sup>c</sup>, Arul M. Varman <sup>c</sup>, Arvind Lali <sup>b</sup>, Reena Pandit <sup>a,\*</sup>

- <sup>a</sup> DBT-ICT Centre for Energy Biosciences, Institute of Chemical Technology, Matunga, Mumbai 400019, India
- <sup>b</sup> Department of Chemical Engineering, Institute of Chemical Technology, Matunga, Mumbai 400019, India
- <sup>c</sup> Chemical Engineering Department, School for Engineering of Matter, Transport and Energy, Arizona State University, Tempe, AZ 85287, USA

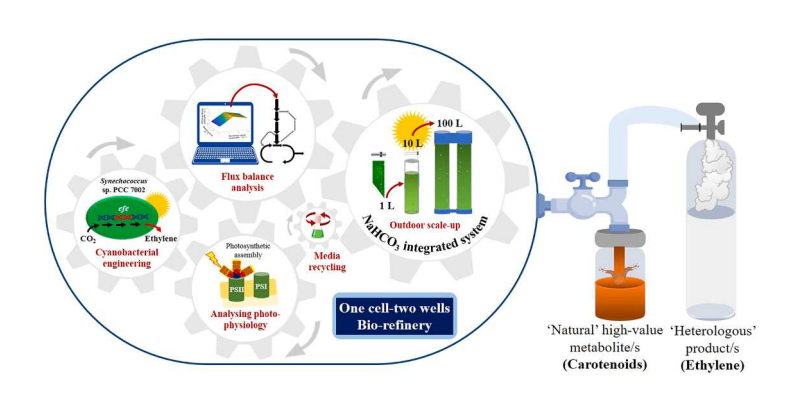
#### HIGHLIGHTS

- Synechococcus was demonstrated to coproduce heterologous and natural hydrocarbons.
- Ethylene (heterologous) and carotenoids (natural) productions improved outdoor.
- Flux balance analysis displayed C<sub>i</sub> supplementation for effective cell sustenance.
- 20 g/L bicarbonate improved PCC 7002 growth and photosynthesis under natural light.
- Outdoor PCC 7002 scale-up cultivation in 100 L system exhibited improved production.

# ARTICLE INFO

Keywords:
Bicarbonate-integrated system
Cyanobacterial Outdoor scale-up cultivation
Flux balance analysis
Ethylene
Carotenoids

#### GRAPHICAL ABSTRACT



# ABSTRACT

In order to improve the potential of cyanobacterial cell factories, Synechococcus sp. PCC7002 was engineered as 'one cell-two wells bio-refinery', for ethylene ('heterologous' hydrocarbon) and carotenoids ('natural' metabolites) production, and demonstrating its outdoor performance. Although the cultures showed better production outdoor, they experienced multiple collapses during scale-up. Hence, flux balance analysis was performed which predicted higher ethylene production with increase in carbon input under outdoor light conditions. Furthermore, FBA predicted that ethylene production will not increase beyond a threshold carbon input flux, owing to limitations on ribulose-1,5-bisphosphate regeneration. Hence, a bicarbonate-supplementation strategy was devised. Cultures grown outdoor at optimal bicarbonate concentration (20 g/L) resulted in improved growth (0.141/h) and ethylene productivity (1.88 mL/L.h) for > 10 days, with enhanced carotenoid titres (40.4 mg/L). In a 100 L air-lift photo-bioreactor; cultures exhibited efficient ethylene (2.464 mL/L.h) and biomass (0.3 g/L.d) productivities, and carotenoids titres (64.4 mg/L), establishing a significant step towards commercialization.

<sup>\*</sup> Corresponding author at: DBT-ICT Centre for Energy Biosciences, Institute of Chemical Technology, Mumbai 400019, India. *E-mail address*: drreenapandit@gmail.com (R. Pandit).

Contributed equally as co-authors.

#### 1. Introduction

Rapid modernization has a profound impact on society's dependency on chemical products derived from petrochemical feedstock. However, for many of such products, their extraction and use, causes global outrage over climate changes, especially due to the increasing accumulation of greenhouse gases (GHGs) (Chi et al., 2013; Zhu et al., 2020, Hajinajaf et al., 2022). Ethylene is one such major building block petrochemical produced worldwide with versatile application in chemical industries. Under the current scenario, ethylene production is majorly practiced by energy-intensive and environmentally detrimental fossil-based steam cracking of naphtha or thermal cracking of ethane (Ghanta et al., 2014). Overall, the environmental impacts to produce ethylene using conventional methods are non-sustainable and thus, mandate alternative "greener" routes for its production. Therefore, global efforts are ongoing for engineering photosynthetic platforms like cyanobacteria for ethylene production.

However, exploiting such potential platforms, just as a 'single product bio-refinery' would render them economically non-viable. Hence, a profitable strategy needs to be devised to maximize biomass utilization and minimize waste generation. A complete value addition to the process could be achieved through holistic deployment of the cvanobacterial system for production of heterologous hydrocarbons as well as natural high-value metabolites, as through 'one cell- two wells biorefinery' approach. Another important factor that could be independently limiting the commercial translation of cyanobacterial candidates, is a scarcity of scientific demonstrations of their performances under natural dynamic conditions, at industrially feasible scales. Therefore, a robust cyanobacterial system could be employed for an effective demonstration. Additionally, there are several reports on ethylene production from fresh water cyanobacteria like Synechococcus elongatus PCC 7942 and Synechocystis sp. PCC 6803 (Carbonell et al., 2019; Durall et al., 2020; Xiong et al., 2015), however marine cyanobacteria, despite being sturdier candidates, remain relatively less explored for the same.

Comprehending these attributes and bottlenecks, under current investigation, we have engineered a euryhaline cyanobacterium *Synechococcus* sp. PCC 7002 (hereafter PCC 7002) for ethylene production by incorporating codon optimized *efe* gene using an in-house plasmid, pUKD6. Simultaneously, natural carotenoids production from the system have been evaluated, especially  $\beta$ -carotene and zeaxanthin. Interestingly, due to lack of lutein biosynthesis pathway, unlike eukaryotic phototrophs, PCC 7002 produces lutein-free zeaxanthin, which otherwise costs around USD 875/ mg of pure zeaxanthin (Sarnaik et al., 2019a; Sarnaik et al., 2019b). In addition, PCC 7002 is a robust system to tolerate dynamic environmental changes like temperature, salinity, high-light, and nutrient supply (Ludwig and Bryant, 2012).

From scale-up cultivation perspective, our group has recently established a successful progressive transition of an engineered fresh water cyanobacterium (Synechococcus elongatus PCC 7942) up to 100 L scale under natural dynamic conditions (Sawant et al., 2021). Although the underlying principle for PCC 7002 scale-up cultivation would be similar as that of PCC 7942, independent set of genetic engineering toolbox, media engineering, and scale-up optimizations were required, as both the systems are metabolically distinct, especially while responding to dynamic environmental changes (Sawant et al., 2021). Further, to identify plausible solution for avoiding culture collapse during volumetric scale-up, in silico flux balance analysis (FBA) was performed. Based on FBA outcomes, carbon supplementation strategy was developed and optimized. Its positive implications were prominently observed through improved cellular photosynthetic efficiency, cell sustenance and enhanced ethylene as well as carotenoids productivities by several folds during outdoor cultivation from 10 to 100 L in photo-bioreactors (PhBRs), without compromising on the biomass. Collectively, in this research, efforts have been made to maximize the utilization of PCC 7002 as a cyanobacterial feedstock through 'one celltwo wells bio-refinery' approach, starting from metabolic engineering to its scale-up optimization, to suit industrial requisites.

#### 2. Materials and methods

#### 2.1. Chemicals & reagents

T4 DNA ligase and restriction enzymes were purchased from New England Biolabs. PrimeStar Max DNA polymerase (2X) high fidelity PCR master-mix was purchased from *Clontech* (DSS TaKaRa Bio India Pvt. ltd.), DreamTaq polymerase by *Thermo Fisher Scientific*, and *TOPreal*<sup>TM</sup> qPCR 2X premix was purchased from *Enzynomics Co. ltd.* (*AllianzBio*, Mumbai, India). *NucleoSpin*® Gel and PCR clean-up kit were purchased from *Macherey-Nagrel* (*MN*, India). Plasmid extraction Miniprep kit was purchased from *GeneAll* (*AllianzBio*, Mumbai, India). Salts and antibiotics were purchased from *Himedia*<sup>TM</sup>.

# 2.2. Culture conditions

PCC 7002 cells were grown in MN (marine nutrient medium, a semi-defined ATCC Medium 957 with 250 mL distilled water, 750 mL seawater, 0.04 g MgSO<sub>4</sub>.7H<sub>2</sub>O, 0.02 g CaCl<sub>2</sub>·2H<sub>2</sub>O, 0.75 g NaNO<sub>3</sub>, 0.02 g K<sub>2</sub>HPO<sub>4</sub>.3H<sub>2</sub>O, 0.003 g Citric acid, 0.003 g Ferric ammonium citrate, 0.0005 g Na<sub>2</sub>-EDTA, 0.02 g Na<sub>2</sub>CO<sub>3</sub>, 1 mL trace metal solution A-5 (2.86 g/L H<sub>3</sub>BO<sub>3</sub>, 1.81 g/L MnCl<sub>2</sub>·4H<sub>2</sub>O, 0.222 g/L ZnSO<sub>4</sub>.7H<sub>2</sub>O, 0.39 g/L NaMOO<sub>4</sub>·2H<sub>2</sub>O, 0.079 g/L CuSO<sub>4</sub>.5H<sub>2</sub>O, 0.049 g/L Co(NO<sub>3</sub>)<sub>2</sub>·6H<sub>2</sub>O) in a 1 L system). Cultures were maintained in an incubator (I<sub>55</sub>) equipped with artificial white cool light illuminated continuously for the fixed light intensity of 55  $\pm$  5  $\mu$ mol/m².s; temperature 30  $\pm$  2°C and mixing at 150 rpm.

# 2.3. Construction of molecular vector for transformation

A recombinant integrative plasmid pUKD6 was constructed for engineering PCC 7002. pUC19 was used as a backbone plasmid containing *E. coli* origin of replication (*ori*), multiple cloning site (MCS), and ampicillin resistance cassette (*Amp'*). pUKD6 was constructed with four fragments, where 750 bps fragments amplified from PCC 7002 genome corresponding to loci SYNPCC 7002\_A0935 as 5'-upstream flanking region (UFR) and SYNPCC 7002\_A0937 as 3'-downstream flanking region (DFR), kanamycin-resistant cassette (*Kan<sup>R</sup>*) from pET28 (+), incorporated into pUC19. Steps for constructing the vector are depicted in the supplementary information (see supplementary files).

pUKDY6 plasmid, with *eyfp* reporter gene cloned in pUKD6, was used to estimate its transformation efficiency under varying conditions: differential plasmid loading (0.5, 1, 2, 4 µg), different topology (*Sac*I digested and linearized, and undigested circular pUKDY6), incubation condition (light or dark, and with differential incubation durations of 6 h and 20 h), and varying initial culture density ( $3 \times 10^7$ ,  $3 \times 10^8$ ,  $3 \times 10^9$ ,  $3 \times 10^{10}$  cells/ mL) (see supplementary files). The optimized culture conditions were further used for transforming pUKED (pUKD6 with *efe* gene under  $P_{trc}$  promoter) (Sawant et al., 2021). The PCC 7002 strain constructed was termed '*syn72\_efe*'. The wild type (WT) and the transformants (Tr), especially *syn72\_efe* were subjected to culture maintenance conditions.

# 2.4. Experimental design under different growth conditions and in photobioreactors (PhBRs)

The WT as well as the Tr, were maintained, acclimatized, cultivated, and evaluated under varying light, temperature, and mixing conditions, as follows:

1. Artificial light condition (A $_{250}$ ): a stand stacked with an array of 32 W tube-lights synchronized to illuminate fixed light intensity of 250  $\pm$  5  $\mu mol/m^2.s$  programmed with light: dark cycle (12:12 h) and temperature 30  $\pm$  2 °C. The 1 L PhBR system was made using a polyethylene sleeve (Heena plastics, India, diameter-147 mm, height-0.05 m, light

transmission- 85 %). The sleeve was provided with a slant geometry at the bottom to ensure a flow pattern for culture suspension and circulation. The spargers were connected at the bottom of the reactor for the suspension of culture.

2. Environmental laboratory-natural light condition ( $E_{1200}$ ): a state-of-the-art temperature-regulated glasshouse facility supporting the cultivation of algae under sunlight with light intensity reaching maximum up to  $1200\pm300~\mu\text{mol/m}^2$ .s with natural diurnal variations; temperature  $30\pm2~^\circ\text{C}$  was used for volumetric scale-up cultivation of the transformants from 1 L PhBR polyethylene sleeve to 10 L PhBR UV-resistant polycarbonate tube. The reactor was supported by poly-vinyl chloride (PVC) joint machined at the bottom and the sparger was set at the bottom for aeration.

3. Outdoor natural light cultivation condition ( $O_{1500}$ ): an outdoor cultivation facility, wherein the cultures were cultivated under sunlight with the maximum light intensity reaching up to  $1500 \pm 300 \ \mu mol/m^2$ .s and temperature  $38 \pm 5$  °C. An external loop airlift photobioreactor (100 L) with a UV-resistant polycarbonate tube (diameter-147 mm, height- 2.8 m, light transmission- 91 %) was used for outdoor cultivation studies with transformants. The system is comprised of a riser and a downcomer, as parallel vertical tubes interconnected with HDPE bottom and top connectors. The sparger aeration was set, where the bottom connector was machined to the central bottom part of the riser. The controlled air flow was provided through a rotameter and mechanical valve to all PhBRs.

Cultures were cultivated using the above-mentioned growth conditions with initial culture densities of  $OD_{730}$  0.4, aeration rate of 0.05 vvm at all the working volumes of 1 L, 10 L, and 100 L in MN medium in a batch mode for upto 10 days. The transformants were monitored and assessed for cell sustenance, biomass growth, biomass productivity, photosynthetic efficiency and ethylene production at predetermined time intervals.

Culture density was determined in terms of  $OD_{730}$  as well as dry cell weight (DCW). For determining DCW, 10 mL culture was harvested in a centrifuge tube and centrifuged at 10,000 rpm for 10 mins. The supernatant was discarded and the pellet was washed twice with distilled water. The biomass was transferred to pre-weighed microcentrifuge tubes, dewatered, and dried in a hot air oven at 60–65 °C for 18 h (Sarnaik et al., 2017). The culture-specific growth rate was determined as a slope of a logarithmic growth phase.

# 2.5. Computational modelling

# 2.5.1. Genome-Scale metabolic model

Flux Balance Analysis (FBA) studies were undertaken using COBRA Toolbox (v2.28) (Schellenberger et al., 2011), running in MATLAB R2020a environment (MathWorks, Inc., Natick, Massachusetts, USA) and the linear programming solver, *glpk*, was utilized to solve for fluxes. An updated PCC 7002 genome-scale model, *i*Syp821 reconstructed by Qian et al. was used (Qian et al., 2017). To simulate the ethylene production in PCC 7002, the reaction for ethylene production was added to this model, as follows (Zhu et al., 2015):  $3\alpha$ -KG + 3  $O_2$  + L-arginine  $\rightarrow 2$  ethylene + 3  $CO_2$  + succinate + guanidine + (S)-1-P5C + 3  $H_2O$ , where  $\alpha$ -KG stands for  $\alpha$ -Ketoglutarate, a key precursor for ethylene synthesis and (S)-1-P5C is abbreviated for 1-pyrroline-5-carboxylate, a metabolite involved in degradation and synthesis of proline (Qamar et al., 2015). The resulting model consisted of 797 reactions, 778 metabolites and 822 genes. Simulations were performed by varying biomass and  $CO_2$  uptake fluxes using an objective function for maximizing the ethylene flux.

# 2.5.2. Constraints employed in the model

The genome scale model, iSyp821, was subjected to several constraints. Bicarbonate uptake flux was set to 0 mmol/gDCW.h at a high light intensity while  $CO_2$  uptake flux was varied from 2 to 8 mmol/gDCW.h. The adenosine triphosphate (ATP) utilization of 1.3 mmol ATP/gDCW.h was used as basal maintenance (Zilliges et al., 2013),

while hydrogen and proton transport were set to 0 mmol/gDCW.h. All other carbon fluxes (such as glucose, acetate, glycerol, glutamate), as well as amino acids exchange and transports, were set to zero and a minimum oxygen uptake rate of 15 mmol/gDCW.h was selected. Other reactions retained the default constraints provided for *i*Syp821 (Qian et al., 2017).

#### 2.5.3. Calculations for photon flux

From outdoor bio-production perspective, light intensity of 1500  $\mu$ mol/m².s (Fig. 3C) was used for calculations. The following assumptions were made to calculate the photon flux input to the cells: (1) Only 45 % of the incident sunlight was absorbed by the cells; and (2) a 9 % theoretical energy conversion efficiency of solar-to-biomass was assumed (Melis, 2009). Based on this, the photon flux rate was calculated as; *Photon flux* =  $1.017 L.r^2/W$ ; where photon flux is in mmol/gDCW.h, L is light intensity in  $\mu$ mol/m².s, r is the radius of a cyanobacterial cell in m, and W is the weight of one cyanobacterial cell in gram (see supplementary files). Assuming PCC 7002 to be a sphere with a cell size of 1  $\mu$ m and a weight of 5.4 pg, the photon flux of 285 mmol/gDCW.h was obtained by using above equation. Hence, the photon flux in iSyp821 was constrained to 285 mmol/gDCW.h.

#### 2.6. Optimization of inorganic carbon supplementation

At a higher scale, the demand for  $\mathrm{CO}_2$  increases exponentially while its availability solely depends upon  $\mathrm{CO}_2$  dissolution in a liquid medium. Supplementing inorganic carbon in the form of bicarbonate could efficiently support the carbon demands at a higher scale (Chi et al., 2013). Therefore, a bicarbonate screening experiment was conducted with  $syn72\_efe$  by supplementing varying concentrations of sodium bicarbonate (0, 2.5, 5, 10, 20 and 40 g/L) in MN medium under  $A_{250}$  and  $E_{1200}$  using 1 L PhBRs, and ethylene productivities were evaluated. All experiments were carried out in triplicates. The culture growth was monitored on daily basis as absorbance  $A_{730}$  using UV–vis spectrophotometer (Shimadzu, UV-2550) and measuring Chl-a content as described by Sarnaik et al. (2017) (Sarnaik et al., 2017). Optimized bicarbonate concentration was selected for further scale-up studies.

# 2.7. Scale-up cultivation of syn72\_efe

<code>syn72\_efe</code> were cultivated under E $_{1200}$  conditions in 1 L PhBR for three consecutive growth cycles in MN medium, with and without 20 g/L bicarbonate. The scale-up transition from 1 L to 10 L PhBR was studied for cell sustenance, biomass, and ethylene productivity. Subsequently, after successful acclimatisation in 10 L PhBR in bicarbonate integrated MN medium for three consecutive growth cycles, <code>syn72\_efe</code> culture was scaled up to 100 L PhBR in O $_{1500}$  and monitored for its growth, photophysiology, and ethylene productivities.

#### 2.8. Analytical methods

# 2.8.1. Gas chromatography-mass spectroscopy for ethylene measurement

For determining ethylene productivity, 8 mL of the culture was transferred into glass vials leaving 12 mL of headspace and crimp-capped them. The gaseous phase was sampled using headspace sampler (G1888 Network Headspace Sampler, *Agilent Technologies*) coupled with GCMS (5975C with triple quadrupole axis detector, inert XL El/Cl MSD, *Agilent Technologies*), where zone temperatures were adjusted for oven at 50 °C, loop and a transition line at 100 °C. Event parameters were adjusted as GC cycle time 1 min, vial equilibration time 0.2 min, pressurization time 0.1 min, loop fill time 0.05 min, loop equilibration time 0.05 min, and injection time 0.2 min. GC (7890A, *Agilent Technologies*) injector temperature was maintained at 40 °C with the detector temperature at 200 °C. The oven ramping was 40 °C for 2 mins, at a rate of 2 °C/min until it reached to 80 °C, where it was held for 2 mins. Helium was used as the carrier gas at a flow rate of 1 mL/min.

For obtaining the ethylene standard curve, the glass vials were filled with 8 mL of MN medium and saturated with ethylene. 1 mL of the gas phase was transferred from the saturated vial to another crimp-capped glass vial with 8 mL MN medium, using a gas-tight Hamilton syringe. Different volumes (1–10  $\mu$ L) of ethylene were injected and the standard curve was plotted as AUC versus ethylene volume. Ethylene productivity was calculated based on its density (1.18 kg/m³) and molar mass (28.05 g/mol).

# 2.8.2. Pulse amplitude modulated (PAM) fluorometry analysis

The PSII and PSI activities were measured in PCC 7002 using dualwavelength pulse-amplitude-modulated fluorometry (Dual-PAM-100, Heinz Walz GmbH, Effeltrich, Germany). A 2 mL culture with OD730 of 1.0 was sampled, which was incubated in the dark for adaptation for 10 mins to allow for measurement of dark respiration. The PAM analysis for syn72\_efe cells was performed using optimized protocol during earlier studies (Sawant et al., 2021). The minimal fluorescence (F<sub>0</sub>) was calculated using a modulated measuring beam of 3  $\mu$ mol/m<sup>2</sup>.s. The actinic light pulse provided was calculated according to photon flux densities (PPFDs) recorded during sampling time. Maximal fluorescence in the dark-adapted (F<sub>m</sub>) and light adapted (F<sub>m</sub>) states were recorded pre- and post-addition of the actinic pulse (1 s) of saturating white light. The quantum yield of energy conversion in PSII i.e Y(II) was calculated as described by Wang et al. (Wang et al., 2015). ETR(I) and ETR(II) were descriptive parameters for electron transport from PS(I) and PS(II). These parameters were derived using the Dual-PAM100 software reflecting the physiological effect of syn72\_efe.

#### 2.9. Carotenoid analysis

The culture density was adjusted to  $OD_{730}$  of 1.0, followed by pigment extraction using methanol (Sarnaik et al., 2017). The filtered pigment extract was used for HPLC analysis of carotenoids with Agilent eclipse XDB  $C_{18}$  RP column. The protocol was derived from study as described by Sarnaik *et al.*, Mobile phase A was methanol: acetonitrile: water (21:16.5:62.5) with 10 mM ammonium acetate and B was methanol: acetonitrile: Ethyl acetate (50:20:30). The solvent B gradient program (time [min], %B, flow rate [mL/min]) was employed as follows: 0, 20, 0.750; 10, 70, 1.0; 40, 100, 1.0; and 60, 100, 1.0, with the absorbance being taken at 480 nm (Sarnaik et al., 2018). Standard curves were plotted for zeaxanthin and carotenoids (Sigma-Aldrich) at 480 nm. Concentrations were calculated as  $(A_{480} \times 4) \mu g/mL$  based on the standards procured from Sigma-Aldrich (Sarnaik et al., 2017).

#### 2.10. Statistical analysis

All the experiments were carried out in biological triplicates while 100 L PhBR studies were performed with technical replicates. The results were expressed as their arithmetic mean and error bars were denoted as the standard deviation (SD). The statistical differences were obtained by single-factor analysis of variance using Microsoft Excel.

# 3. Results & discussion

Huge increase in atmospheric GHGs like  $\mathrm{CO}_2$  is a global concern and hence, driving more attention towards cyanobacterial cell factories from hydrocarbon production and concurrent  $\mathrm{CO}_2$  mitigation perspectives. Though many studies have attempted green synthesis of hydrocarbons like ethylene using engineered cyanobacteria, it remains unexplored for its commercial appeal. Among several factors limiting its commercialization; choice of a sturdy host system, deficiency of outdoor cultivation studies, strategy development for maximal biomass deployment, and formulation of economical and efficient culture media; are the predominant ones. Therefore, the present study could be regarded as a holistic demonstration to leverage a cyanobacterial system for industrial translation.

#### 3.1. Genetic engineering of PCC 7002

PCC 7002 was genetically engineered using integrative backbone vector pUKD6. The vector was constructed using 2-step single overlap extension PCR and restriction cloning. The successful vector assembly was confirmed by gel electrophoresis (see supplementary files). The expression vector, pUKDY6 was transformed in PCC 7002 and was evaluated for its transformation efficiency (see supplementary files). Results exhibited the highest transformation efficiency by adding 1  $\mu g$  of the plasmid (linear or circular) DNA with 3  $\times$  10 $^8$  cells/mL and incubating in light, overnight (see supplementary files). Constitutive eYFP expression was confirmed by comparing the fluorescence of WT and Tr for 10 days (see supplementary files). The Tr exhibited significant eYFP fluorescence over WT, indicating successful heterologous gene integration and constitutive expression. The optimized transformation conditions were employed for transforming pUKED plasmid (with efe) into PCC 7002 for the ethylene production. Positive colonies of syn72 efe were selected after subsequent confirmation using colony PCR (see supplementary files). Ethylene production was estimated using GC-MS, where the results showed 50 µL/L.h and 0.086 g/L.d of ethylene and biomass productivities, with 1.8 mg/L and 0.72 mg/L of β-carotene and zeaxanthin, respectively, at 55 µmol photons/m<sup>2</sup>.s, in the incubator, I<sub>55</sub>. These preliminary experiments confirmed successful PCC 7002 engineering. Hence, syn72\_efe was proceeded for natural light cultivation and subsequent scale-up.

# 3.2. Growth of engineered PCC 7002 under natural light conditions

While working with photosynthetic chassis, light intensity and exposure have a significant influence on the overall sustainability prospect, especially during scale-up cultivation (Sarnaik et al., 2019a; Sarnaik et al., 2019b, Sarnaik et al., 2017). To project sustainability, the use of natural light during cultivation is imperative (Pathak et al., 2018). Cultivation of transformants in outdoor conditions using natural light would mandate their gradual transitioning from maintenance conditions to outdoor dynamic conditions. Such transitioning process involved continuing adaptive evolution of the transformants while addressing cell sustenance, photosynthetic performance and challenges associated with the scale-up cultivation.

PCC 7002 cultures were initially grown using a defined (ASNIII + BG-11, 1:1) (Cumino et al., 2010) and a partially defined (MN) media (www-cyanosite.bio.purdue.edu). Results showed that the culture growth in both the media was equivalent; but considering the cost economics and scale-up feasibility, MN medium (containing 75 % sea water) was used for further experimentation. The transformants maintained in Is5 were progressively acclimatized in E $_{1200}$  under natural light conditions using 1 L reactor and demonstrated a 4-fold increase in specific growth rate (0.11  $\pm$  0.02 /h) compared to Is5.

To understand and address bottleneck/s of culture sustenance during large-scale cultivation, syn72\_efe were grown in 1 L PhBR and then transferred to 10 L PhBR, in E<sub>1200</sub>. In 1 L PhBR, syn72\_efe attained early stationary phase on the 4th day of cultivation, while syn72\_efe cultivated in 10 L PhBR collapsed on the 6th day (see supplementary files). Similar culture collapse was encountered on multiple occasions when grown at 10 L PhBR scale (data not shown). It has been reported that genetically engineered organisms are extremely susceptible to the effect of multiple factors such as contamination, photo-dynamics, nutrient limitations and photo-damage caused due to reactive oxygen species (ROS) and thus prominently observed to crash (Davies et al., 2021; Latifi et al., 2009). It was reported that the contamination was a major causative factor for the culture crash. Therefore, we daily monitored the culture for contamination, and it was observed to be monoalgal, even before the culture crash. Hence, we could speculate the involvement of other parameters during scale-up and subsequent collapses, including inadequate inorganic carbon, and higher light intensities during noon where photo-damage through ROS production could be prominent and

thus could be detrimental. In principle, photosynthetic electron transfer, results in reducing equivalents NADPH and ATP production which are later utilized for carbon fixation in TCA cycle (Xiong et al., 2015). The interdependency of carbon availability and light intensity are regulated by a tighter niche (Knoot et al., 2018) and thus, the overall carbon flux plays a critical role in the metabolic dynamics (Ducat et al., 2012).

Secondly, from the co-production perspective, the theoretical yields were calculated by balancing the stoichiometry of 80 CO<sub>2</sub> and 56 H<sub>2</sub>O to

one Zeaxanthin ( $C_{40}H_{56}O_2$ ), one  $\beta$ -carotene ( $C_{40}H_{56}$ ) and 111  $O_2$ . Strains engineered for ethylene production would require additional 2 mol of  $CO_2$  and  $H_2O$  for 1 mol of ethylene (82  $CO_2 + 58$   $H_2O \rightarrow C_2H_4 + C_{40}H_{56} + C_{40}H_{56}O_2 + 111$   $O_2$ ). Thus, theoretically,  $\sim$ 13.9 g of  $CO_2$  will be required for just 1.11 g of carotenoids ( $\sim$ 1 g of carotenoids/ 12.65 g of  $CO_2$ ), whereas we can produce 28.05 g (23.77 mL) of ethylene from 17.88 g of  $CO_2$  ( $\sim$ 1 g of ethylene/ 1.56 g of  $CO_2$ ). Carotenoid synthesis is indispensable for the cell and requires 8-fold more  $CO_2$  than that for

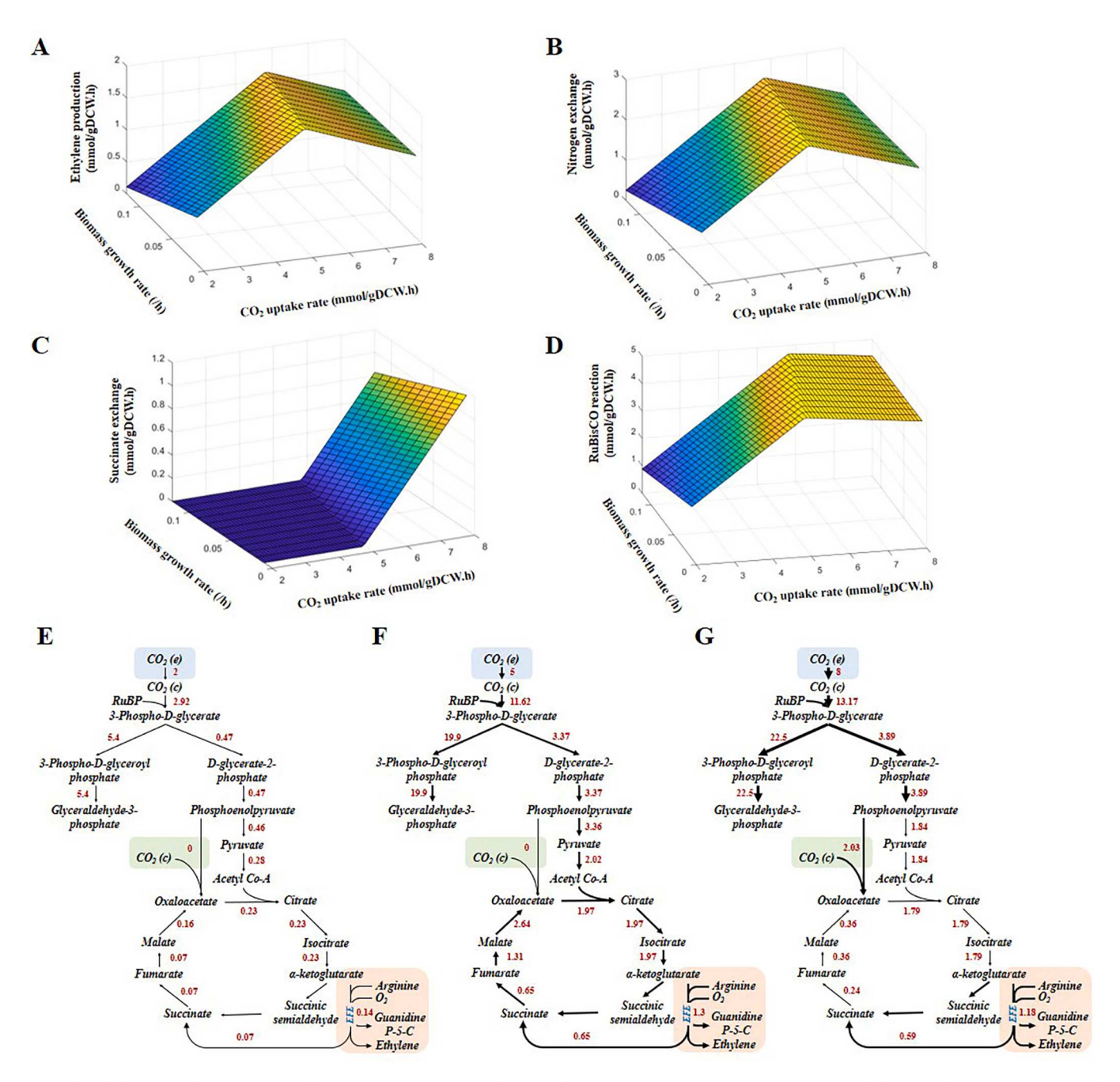


Fig. 1. Flux balance analysis (FBA) for determining inorganic carbon supplementation strategy in PCC 7002. (A) Ethylene production. Increase in inlet bicarbonate increased ethylene production from 1.907 to 5 mmol/gDCW.h  $CO_2$  uptake; beyond which the production was found to have reduced. Biomass production was found to compete with the ethylene production. (B) Nitrogen (ammonium) exchange. The highest ammonium exchange was observed when the ethylene production peaked up. Higher nitrogen flux was needed as more  $\alpha$ -ketoglutarate was used for the synthesis of ethylene and guanidine ( $CH_5N_3$ ). (C) Succinate exchange. Succinate exchange, a by-product of EFE catalysis, was found to increase beyond 5 mmol/gDCW.h  $CO_2$  uptake rate. (D) RuBisCO reaction high  $CO_2$  input combined with natural light conditions reduced regeneration of ribulose-1,5-bisphosphate (RuBP), thereby limiting RuBisCO activity. Pathway fluxes during  $CO_2$  assimilation at (E) 2, (F) 5, and (G) 8 mmol/gDCW.h  $CO_2$  uptake rates have been schematically represented to exhibit their effects on ethylene production. It was seen that ethylene production improved almost 10-fold when  $CO_2$  flux increased from 2 to 5 mmol/gDCW.h, whereas the production reduced at 8 mmol/gDCW.h. Thickness of the arrows corresponds to the reaction fluxes.

ethvlene.

To evaluate such effects, *in silico* flux balance analysis was performed to provide a competent solution and to avoid culture collapses, concurrently improving the co-production.

# 3.3. Flux balance analysis (FBA)

FBA was performed to evaluate the impact of increasing carbon input on ethylene production under outdoor conditions and to gain systems level understanding of the fluxome of the engineered organism. As FBA was used as a predictive tool in this work and as the growth rate of the organism was unknown under natural light conditions, simulations were performed by varying specific growth rates. This would provide insights into the impact of carbon input on the metabolism which could hold true irrespective of the actual growth rate.

The simulations were performed with an objective to maximize the ethylene flux and two distinct phases appeared in the ethylene production charts (Fig. 1A). In phase I, as expected, ethylene production increased with an increase in CO2 input and reached a maximum of 1.625-1.907 mmol/gDCW.h depending on the input CO2 flux and biomass growth rate. However, in a later phase II, ethylene flux kept declining from its maximum despite increasing the input CO<sub>2</sub> flux. Thus, it could be inferred that by increasing the CO2 concentration in the medium, ethylene production could be increased until a threshold value. It is also notable to mention that the maximum ethylene flux at a higher biomass flux, less ethylene is produced which can be attributed to the fact that with a higher biomass flux, less carbon is available for the ethylene production. Although the modelling results would be used for experimental design, this computational calculation of maximum yield should not be regarded as a forecast of actual yield, but rather as a reference point for what was theoretically feasible under ideal conditions.

To verify the decrease in ethylene production during phase II, the flux results were further analysed. In principle, ethylene bio-production is also dependent on the availability of several macro- and micronutrients apart from carbon supply. In this regard, nitrogen is one of the most important elements required for cyanobacterial growth and bio-production. Although it was assimilated in various forms, all forms of nitrogen were ultimately transformed into ammonium inside the cell (Carol potera, 2005). In addition, studies have shown that carbon and nitrogen assimilation are coupled in cyanobacteria through a sophisticated transcriptional regulation system to ensure a carbon/nitrogen metabolic balance (Muro-Pastor et al., 2005). Due to this regulation, nitrogen limitation could have resulted in downregulation of genes involved with carbon concentrating mechanism (CCM), ultimately limiting carbon uptake even if carbon substrate was in oversupply (Muro-Pastor et al., 2005; Zhang et al., 2018). To verify our hypothesis, we investigated the effect of varying CO2 input flux and biomass growth rate on nitrate exchange flux (Fig. 1B). From Fig. 1B, it can be verified that nitrate influx increased from 1.12 to 2.86 mmol/gDCW.h, when the CO<sub>2</sub> flux increased from 2 to 8 mmol/gDCW.h at a biomass flux of 0.01 1/h. Likewise at a biomass flux of 0.12 1/h, ethylene flux reached a maxima of 1.668 mmol/gDCW.h while the CO2 flux was at 5.8 mmol/ gDCW.h. However, as nitrogen flux did not reach the upper limit provided in the model (10000 mmol/gDCW.h), FBA analysis concluded that nitrogen availability did not constrain ethylene production for the given constraints.

To further investigate the factor that limited the production of ethylene, succinate exchange flux was investigated (Fig. 1C). Interestingly, although succinate is a by-product of the ethylene formation reaction, succinate flux did not follow the same pattern as ethylene flux. Instead, succinate exchange exhibited no flux when  $CO_2$  influx and biomass flux were varied from 2 to 5 mmol/gDCW.h and 0.01 to 0.12 1/h respectively. As the  $CO_2$  flux was increased further succinate flux started to increase and reached a maxima of 1.16 mmol/gDCW.h at a  $CO_2$  flux of 8 mmol/gDCW.h. At high  $CO_2$  flux, oxaloacetate was

produced by PEP carboxylase which led to an increase in succinate pool and thereby resulting in an increase in succinate exchange out of the cell (Fig. 1E-G). The reason lies in the fact that at CO<sub>2</sub> influx of 2 or 5 mmol/ gDCW.h, there is no flux from phosphoenolpyruvate (PEP) to oxaloacetate, while at CO2 influx of 8 mmol/gDCW.h, a flux of 2.03 mmol/ gDCW.h from PEP to oxaloacetate is observable. Basically, at lower CO2 flux, succinate was produced as a by-product of ethylene reaction, but the succinate was converted to oxaloacetate through subsequent reactions thereby minimizing succinate exchange. Thus, FBA analysis concluded that high CO2 input combined with natural light conditions reduced regeneration of ribulose-1,5-bisphosphate (RuBP) (Fig. 1D), thereby limiting the ability of the cell to fix CO2 by RuBisCO (Dokulil, 2022). The overflow of input CO2 was fixed by PEP carboxylase ultimately limiting carbon availability for ethylene production. Fig. 1E-G show the flux map of carbon from CO<sub>2</sub> to the final products of succinate and ethylene.

# 3.4. Effect of bicarbonate-integrated approach in performance sustenance of transformant

As envisaged earlier, culture supplementation with an additional inorganic C like CO<sub>2</sub> was necessary from the production perspective. In conventional microalgal cultivation systems, CO2 is supplied by sparging CO<sub>2</sub> enriched air to the medium. This method could be a costly affair when factors like transportation, storage, purification, equipment for sparging, and energy expenditure to drive this equipment are taken into consideration (Chi et al., 2013). For cost-effectiveness, bicarbonatebased cultivation can be envisioned (Zhu et al., 2021). This system has potential advantages apart from reducing cost and energy inputs, which are indispensable for compression, purification, transportation and storage of CO2. Sodium bicarbonate has been known to provide buffering activity. Secondly, as HCO3 ions are symported with Na+, Na+ gradient is usually restored through H+ mediated antiports (Forchhammer and Selim, 2019) (Fig. 2). This ultimately reduces the extracellular H<sup>+</sup> ions concentration rendering the medium alkaline. Alkaline pH, in addition, helps in controlling the potential media contamination (De Farias Silva et al., 2017; Mangan et al., 2016). Comprehending these advantages, the bicarbonate-integrated system could be implemented to an array of phototrophic systems (Chi et al., 2014; Zhang et al., 2019; De Farias Silva et al., 2017). Additionally, bicarbonate counters oxidative stress by effective mediation of electron transfer between plastoquinone (PQ) to cytochrome bef by regulating quinone (QA), therefore acting as a bidentate ligand to bridge electron transfer (Shevela et al., 2020), contemplating its role in cultivation.

Hence, to restore the carbon inadequacy during the scale-up cultivation and as directed through FBA, the cultures were supplemented with sodium bicarbonate to enhance cell fitness and productivity (Chi et al., 2014; Zhang et al., 2019). Preliminary experimentation was performed with ambient air (0.04 % v/v CO<sub>2</sub>) and 5 g/L bicarbonate integrated system (Sawant et al., 2021). Results exhibited prominent improvement in the biomass and ethylene productivities along with total carotenoid titres in bicarbonate supplemented cultures over the ones grown with ambient air bubbling (Fig. 2, bar graphs). Therefore, as a next step, bicarbonate concentration optimization for improved biomass and ethylene productivities was evaluated over the period of 10 days.

#### 3.5. Optimization of bicarbonate supplementation strategy

In cyanobacteria, bicarbonate is the ultimate form of inorganic carbon uptaken by the carboxysomes and converted to  $\mathrm{CO}_2$  by virtue of enzyme carbonic anhydrase, which will be further assimilated by RuBisCO through Calvin-Benson-Bassham (CBB) cycle into glucose (Mangan et al., 2016) (Fig. 2). This anabolism is followed by a central metabolic pathway that ultimately forms pyruvate. Although generally, pyruvate enters the TCA cycle, cyanobacteria like PCC 7002 have

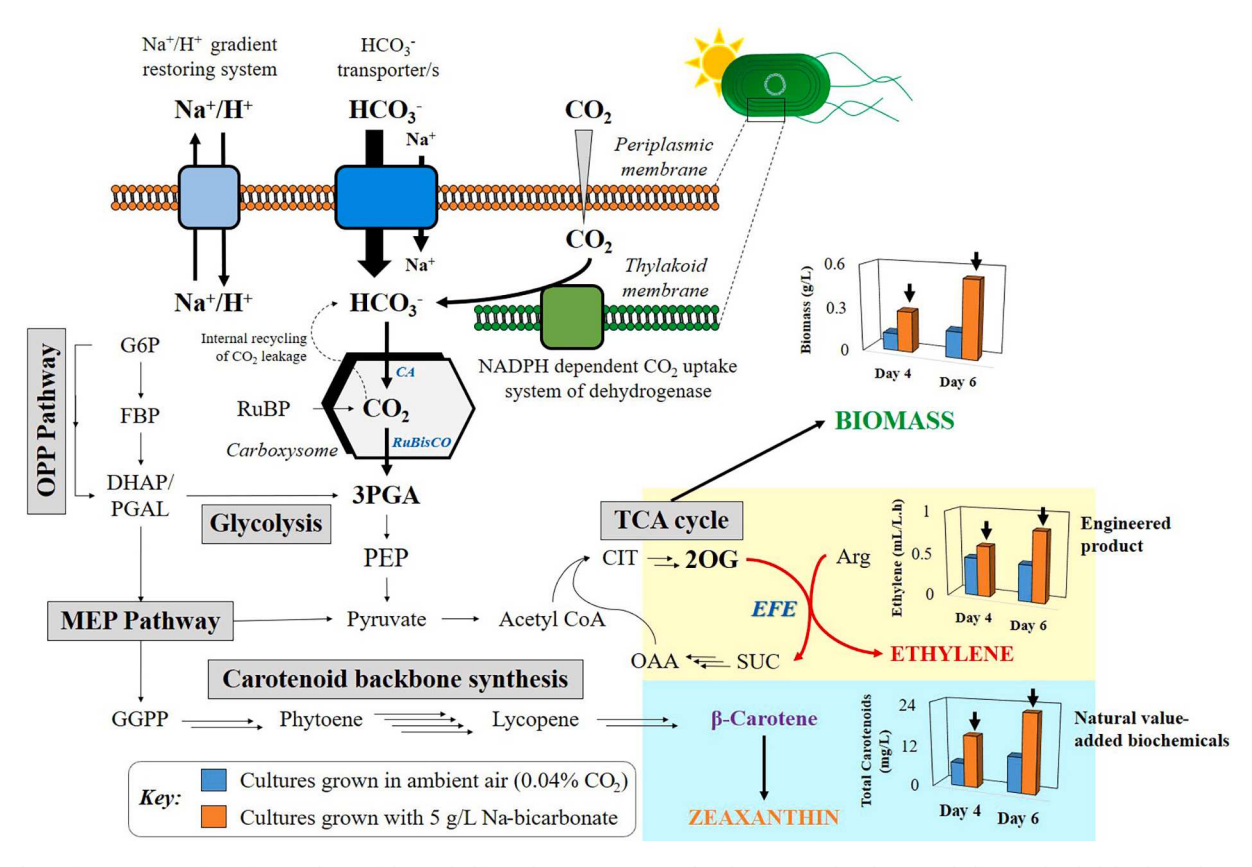


Fig. 2. Schematic representation of cyanobacterial metabolism where,  $CO_2$  is assimilated into central carbon metabolism at the thylakoid membrane through NADPH based reduction to  $HCO_3^-$ , and  $HCO_3^-$  as an independent substrate is assimilated at the periplasmic membrane, especially via  $Na^+$  assisted symport. Comparative evaluation of cultures grown under ambient air and 5 g/L bicarbonate supplementation indicated improved production with bicarbonate. Data collected in biological triplicates, n=3, and shown as mean  $\pm$  SD, p>0.01.

incomplete TCA cycle. Therefore, 2-oxoglutarate (2-OG or α-ketoglutarate) becomes terminal compound of the citrate pathway, and it is usually replenished through various salvage pathways including nitrogen metabolism (Zhang et al., 2018). In our engineered strain, 2-OG would have two fates: biomass and ethylene production. Hence, an increase in bicarbonate supplementation would ultimately affect cell growth as well as ethylene productivity. Transformants grown in MN medium with incremental bicarbonate supplementation exhibited an increase in specific growth rate and ethylene productivity, as expected. However, the increase was not consistent. When initial bicarbonate supplementation was increased from 2.5 g/L to 5 g/L, there was an 85 % increase in specific growth rate but only a 65 % increase in ethylene productivity as compared to the un-supplemented control, Fig. 3A. On the other hand, when we moved from 10 g/L to 20 g/L bicarbonate concentration, there was a 55 % increase in specific growth rate but a 95 % increase in ethylene productivity. The highest specific growth rate  $(0.1406 \pm 0.081 \text{ /h})$  and ethylene productivity  $(1.876 \pm 0.085 \text{ mL/L.h})$ were obtained with 20 g/L bicarbonate supplementation to 10 L of the culture under  $E_{1200}$ , Fig. 3A. However, further increase in bicarbonate concentration to 40 g/L reduced the growth rate and ethylene productivity, Fig. 3A, as predicted by FBA. These results indicated that although an increase in bicarbonate concentration supported biomass and ethylene production, the concentration of 2-OG could be one of the decisive parameters in determining the relative carbon flux towards both these products. Secondly, a separate set of studies was performed to evaluate the effect of bicarbonate supplementation on nitrate assimilation by the cells, exhibiting negligible correlation, as suggested by FBA (see supplementary information). However, separate metabolomic investigations need to be conducted to test this hypothesis.

Transformants grown in MN medium supplemented with 20 g/L

sodium bicarbonate exhibited not only sustained longer growth cycles with delayed stationary phase, but also improved the growth rate (Fig. 3B). Furthermore, pH in bicarbonate supplemented medium was found to be retained at  $9 \pm 1$  during cultivation, reflecting the buffering activity of bicarbonate and thereby accounting for improved sustenance of transformant in E<sub>1200</sub>, Fig. 3B (Zhu et al., 2021). Moreover, an increase in pH and K<sub>L</sub>a enhances carbon utilization efficiency (CUE), further indicating that bicarbonate-integrated systems would be a better approach for sustainable cultivation and has been found to significantly lower the biomass costs (Benschop et al., 2003; Ji et al., 2020). Acclimatized syn\_72efe grown in MN medium with an optimized 20 g/L bicarbonate concentration were cultivated in O<sub>1500</sub>, using 100 L PhBR under outdoor dynamic light conditions (Fig. 3C). The syn\_72efe exhibited improved biomass productivity of 0.325  $\pm$  0.136 g/L.d (concentration 3.8  $\pm$  0.2 g/L) and ethylene productivity of 2.464  $\pm$  0.099 mL/L.h, Fig. 3D. Interestingly, like biomass and ethylene, total carotenoid titre was found to improve over  $E_{1200}$  to 64.4  $\pm$  0.07 mg/L. This study is the first that demonstrated ethylene production by engineered PCC 7002 using 100 L PhBR, outdoor.

# 3.6. Media recycling studies

The transformants were cultivated in MN medium with or without (control) 20 g/L bicarbonate under natural light conditions, and the corresponding media were replenished with macronutrient supplementation (750 ppm nitrate and 20 ppm phosphate) after each cycle. The results clearly indicated that despite decrease in the growth over 4 successive recycles for 30 days, the bicarbonate supplemented medium consistently showed higher growth than the un-supplemented one (see supplementary files). Corresponding growth reduction was also

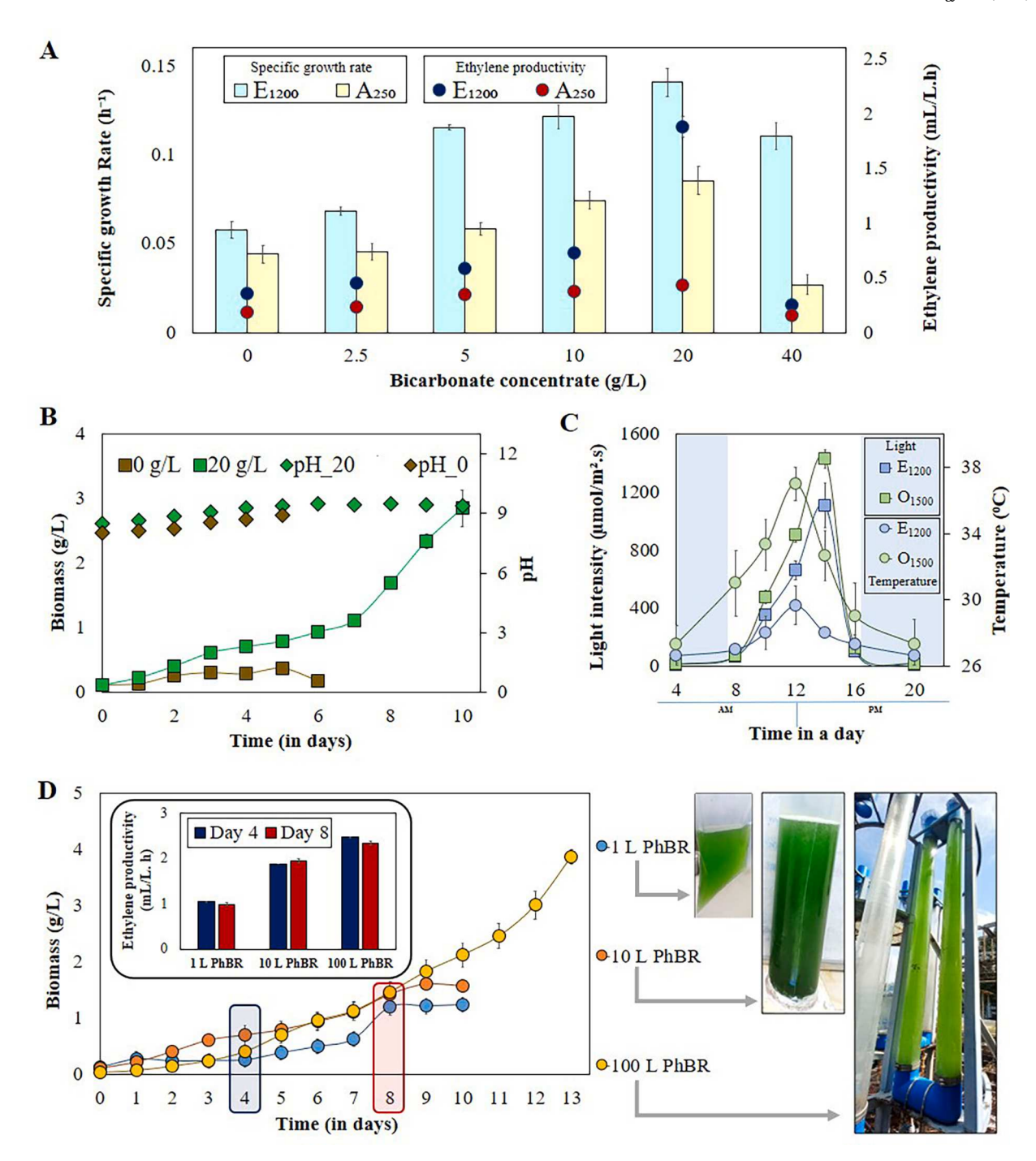


Fig. 3. Effect of bicarbonate-integrated system on culture sustenance, ethylene productivity and volumetric scale-up. (A) Screening of different bicarbonate concentrations in MN medium for specific growth rate (/h) and ethylene productivity (mL/L.h) of Syn\_72efe transformants in  $E_{1200}$  and  $A_{250}$ . The results indicated the highest specific growth rate and ethylene productivity with 20 g/L bicarbonate supplementation in  $E_{1200}$ . (B) Culture sustenance studies in 20 g/L bicarbonate supplemented and un-supplemented (control) MN media. The results prominently exhibited positive effect of bicarbonate supplementation on culture sustenance as well as biomass production. pH monitoring showed pH maintained between 8.5 and 9.0 over 10 days. (C) Variable light intensities ( $\mu$ mol/m².s) and temperatures (°C) at different time in a day in  $E_{1200}$  and  $E_{1200}$  a

observed due to either depletion of macro and micro-nutrients, or a simultaneous build-up of repressing biochemicals into the spent media.

# 3.7. Carotenoid analysis

Apart from the heterologous products, natural high-value metabolites like carotenoids, from the cyanobacterial system could be extracted

through 'one cell – two wells bio-refinery approach' (Sarnaik et al., 2019a; Sarnaik et al., 2019b). This could lead to a complete value-addition to the system. Importantly, unlike eukaryotic photoautotrophs, cyanobacteria are known to synthesize only zeaxanthin and no lutein (Bourdon et al., 2021). Being structural isomers, lutein and zeaxanthin are difficult to separate during downstream processing, with significantly higher lutein fraction in the eluate (Pniewski, 2020).

Therefore, majority of the zeaxanthin-based products have both the carotenoids in varying fractions. Thus, a cyanobacterial system can be well-harnessed for extraction of lutein-free zeaxanthin, which is one of the costliest fine chemicals in its pure form, with relatively higher antioxidant capacity over lutein (Sarnaik et al., 2019a; Sarnaik et al., 2019b, Sarnaik et al., 2018). Besides zeaxanthin, its precursor,  $\beta$ -carotene is an abundant carotenoid from cyanobacteria. Hence, under current investigation, carotenoid analysis was independently performed for the transformants grown in MN medium, with and without bicarbonate supplementation in  $A_{250}$  and  $E_{1200}$  (see supplementary files).

Cultures grown in  $E_{1200}$  with bicarbonate supplementation showed  $13.98 \pm 0.29$  mg/gDCW of  $\beta$ -carotene and  $2.86 \pm 0.09$  mg/gDCW of zeaxanthin yields with  $1.72 \pm 0.07$  mL/L.h of ethylene productivity on the 4th day of cultivation, whereas the ones grown without the supplementation showed  $6.5 \pm 0.35$  mg/gDCW of  $\beta$ -carotene and  $1.55 \pm 0.07$  mg/gDCW of zeaxanthin yields with  $0.45 \pm 0.05$  mL/L.h of ethylene productivity (see supplementary files). The improvement in the yields and productivities were consistent even on the 6th day of cultivation, significantly indicating positive effect of bicarbonate supplementation in development of efficient cyanobacterial bio-refinery, even considering carotenoid production. Further, the carotenoid titres were found to have substantially improved, where bicarbonate supplemented cultures showed 3–4 times higher titres of  $\beta$ -carotene (27.66 mg/L on day 4 and 23.16 mg/L on day 6) and zeaxanthin (4.75 mg/L on day 4 and 6.95 mg/L on day 6) over the un-supplemented ones (Fig. 4).

In principle, zeaxanthin synthesis is triggered when cells encounter physiological stress including high light (Latifi et al., 2009; Sarnaik et al., 2018). Therefore, relative fraction of zeaxanthin over  $\beta$ -carotene (zeaxanthin precursor), could be considered as a measure of response to the cell stress (Faraloni & Torzillo, 2017). In the current study, when syn\_72efe were grown in MN medium with 20 g/L bicarbonate showed relatively less zeaxanthin to  $\beta$ -carotene (Z:B) ratio on the 4th (0.20) and 6th day (0.25) compared to those of the control (0.24 on day 4 and 0.36 on day 6), under natural light conditions, indicating lowering of the physiological stress (see supplementary files). This recapitulates the bicarbonate effect on alleviating such physical stress, improving the cell sustenance, growth rate, and consequently increasing the ethylene productivities and carotenoid titres (Sarnaik et al., 2019a; Sarnaik et al., 2019b). Considering these improvements, MN medium with 20 g/L bicarbonate could be considered as optimum for PCC 7002 outdoor cultivation, and product/s formation.

#### 3.8. Effect of Bicarbonate-based systems on photosynthetic response

Sodium bicarbonate has a dual role to play during photosynthetic electron transfer; as an electron donor and acceptor (Shevela et al., 2020). Mobile bicarbonate acts as proton donor to enhance water oxidation and dissociates into CO2 and H2O. Secondly, it plays a significant role as the electron donor in regulating quinone (QA) during the electron transfer (Shevela et al., 2020), thereby accelerating overall electron transfer. Thus, evaluation of bicarbonate effect on photosynthetic response of transformant in  $E_{1200}$  under natural light conditions would throw more light on the effect of bicarbonate supplementation on the cellular photosynthetic response. In addition, cyanobacteria are known to modulate their photosynthetic response by changing antenna (pigment) density and/or state transition under dynamic light conditions (Kirst et al., 2014; Sarnaik et al., 2017). Therefore, it was paramount to understand acclimatization responses of photosynthetic apparatus and performance threshold on their exposure to natural light conditions.

 $Syn_.72efe$  grown in MN medium under natural light conditions exhibited modulations with Chl-a, where Chl-a content decreased with an increase in light intensities as photo-protective mechanism to reduce photo-oxidative damage (Singh et al., 2009), Fig. 5A. The consequence of this modulation are the changes in overall energy distribution between the two photosystems (PSI & PSII). Therefore, transformants were evaluated for photosynthetic response after adaptation in  $E_{1200}$ , using PAM fluorometry.  $Syn_.72efe$  in mid-exponential phase were analysed at regular intervals for effective PSII quantum yield (Y (II)), electron transport rate at PSII (ETR II), and PSI (ETR I) reaction centres.

With an increase in light intensity beyond saturation, Chl-a content reduces with consequent reduction in Y(II). This could be considered as an effective determinant of photo-adaptability. Y (II) for the transformants grown in 20 g/L bicarbonate exhibited similar circadian pattern; but with improved efficiency over the control (without bicarbonate supplementation), Fig. 5B. Further, the transformants also exhibited a synchronized increase in ETR (I) and ETR (II) activities (Fig. 5C & 5D). This increase in non-cyclic electron flow from PSII with increasing light intensity could be balanced by cyclic electron flow at PSI. The status of cyclic and non-cyclic electron flow revealed the limitation of reducing equivalents generated during photosynthesis (Mullineaux and Emlyn-Jones, 2005), NADPH and ATP. Increased electron flow due to addition of bicarbonate could have countered such limitations during outdoor scale-up cultivation. Thus, there was synergistic

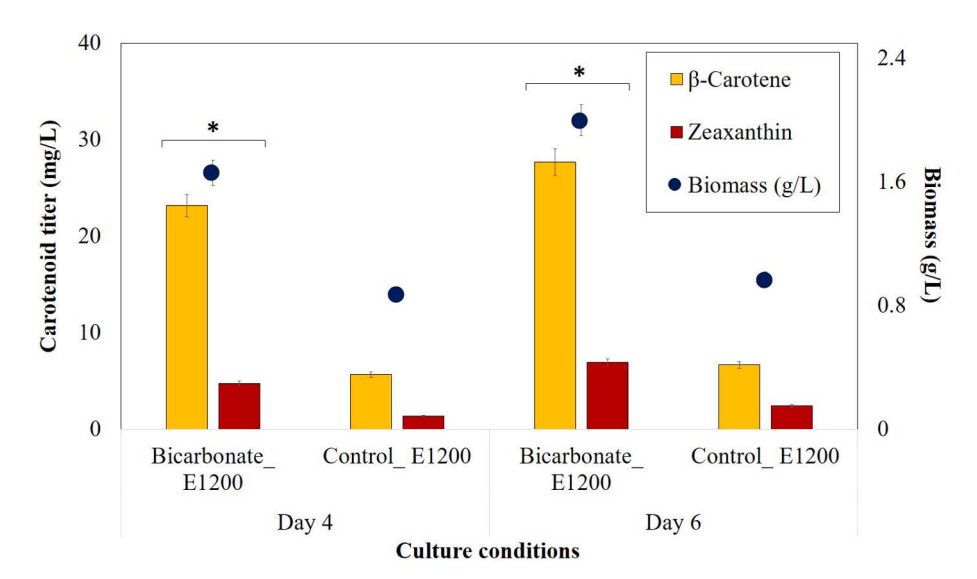


Fig. 4. Comparative analysis of carotenoid (Zeaxanthin and  $\beta$ -carotene) production from Syn\_72efe. Zeaxanthin and  $\beta$ -carotene production was analysed from the transformants grown in MN medium with or without bicarbonate supplementation under natural light conditions. Results indicated significantly high carotenoid content in bicarbonate grown cultures over the control. Data shown as mean  $\pm$  SD, n=3, p>0.01.

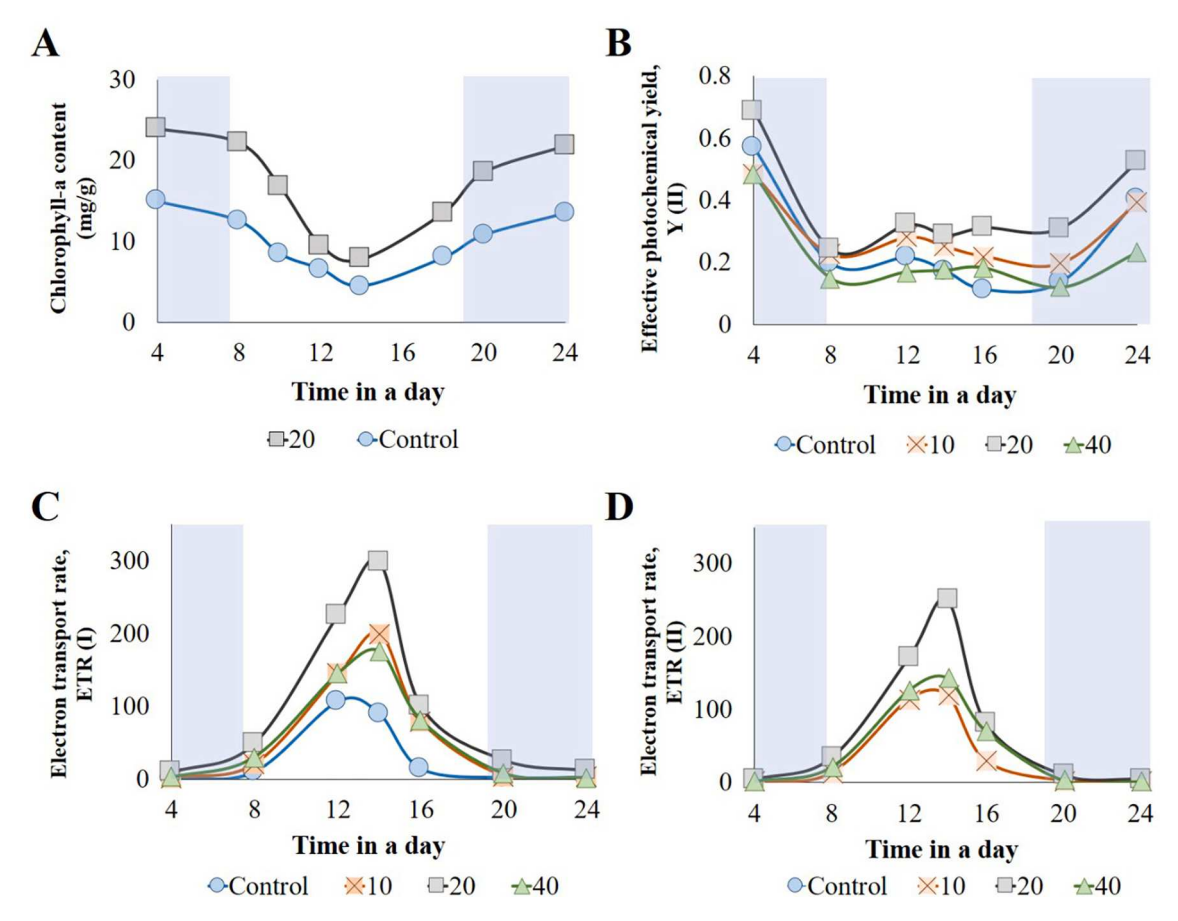


Fig. 5. Photosynthesis responses of transformants grown in bicarbonate-integrated MN medium under natural light conditions using PAM fluorometry. (A) Chl-a content (mg/g) of the transformants over the day, in optimised 20 g/L bicarbonate-integrated system and control. Chl-a content was found to reduce with increase in light intensity and vice versa. Bicarbonate supplemented samples showed consistently higher Chl-a content iover the control. (B) Effective photochemical yield (Y(II)) of the cultures grown with 10, 20 and 40 g/L bicarbonate-supplementation. Y(II) exhibited similar trend as Chl-a, where the highest yields were obtained with 20 g/L bicarbonate. (C) Electron transport from PS I (ETR I) and (D) PS II (ETR II) in E1200 displayed increase in the rates with increase in the light intensity, where 20 g/L bicarbonate supplemented cultures showed the highest rates.

onset of bicarbonate effect, pigment modulation and cyclic electron transport which contributed to improved sustenance and adaptation of transformants under dynamic outdoor conditions.

# 4. Conclusion

We successfully presented one cell–two wells bio-refinery approach for a marine cyanobacterium. For demonstrating industrial feasibility, the approach was successfully exhibited at 100 L scale, under outdoor conditions, giving improved biomass and corresponding heterologous (ethylene) and natural high-value metabolites ( $\beta$ -carotene, zeaxanthin) from PCC 7002. The approach compatibility can be further leveraged by optimizing continuous ethylene extraction at the gas–liquid interface, coagulation-assisted biomass separation, and carotenoid extraction. The use of renewable resources like sunlight, sea-water, carbon-dioxide, could render the process more sustainable. This multi-product bio-refinery approach would be platform-independent and can be extended to other microbes with subsequent amendments.

# CRediT authorship contribution statement

Kaustubh R. Sawant: Conceptualization, Methodology, Validation, Investigation, Writing – original draft, Data curation. Aditya P. Sarnaik: Conceptualization, Visualization, Software, Formal analysis, Writing – review & editing, Supervision, Validation. Prashant Savvashe: Methodology, Validation, Resources, Software. Nima Hajinajaf:

Conceptualization, Visualization, Software, Writing – original draft, Data curation. **Parker Poole:** Software, Writing – review & editing, Data curation. **Arul M. Varman:** Project administration, Writing – review & editing. **Arvind Lali:** Project administration. **Reena Pandit:** Project administration, Supervision, Writing – review & editing.

#### **Declaration of Competing Interest**

The authors declare that they have no known competing financial interests or personal relationships that could have appeared to influence the work reported in this paper.

# Data availability

No data was used for the research described in the article.

# Acknowledgement

The authors acknowledge the Department of Biotechnology, Ministry of Science and Technology, Govt. of India for the support of the work (under grant agreement no. BT/PR 311 55/PBD/26/725/2019 and BT/EB/ICT-Extension/2012). This research was also supported in parts by the National Science Foundation through a grant to A.M.V (CBET-2146114).

#### Appendix A. Supplementary data

Supplementary data to this article can be found online at https://doi.org/10.1016/j.biortech.2022.127921.

#### References

- Benschop, J.J., Badger, M.R., Price, G.D., 2003. Characterisation of CO2 and HCO3-uptake in the cyanobacterium. Photosynth. Res. 117–126.
- Bourdon, L., Jensen, A.A., Kavanagh, J.M., McClure, D.D., 2021. Microalgal production of zeaxanthin Microalgal production of zeaxanthin. Algal Res. 55, 102266.
- Carbonell, V., Vuorio, E., Aro, E.M., Kallio, P., 2019. Enhanced stable production of ethylene in photosynthetic cyanobacterium Synechococcus elongatus PCC 7942. World J. Microbiol. Biotechnol. 35, 1–9. https://doi.org/10.1007/s11274-019-2652-7.
- Carol potera, 2005. Making Succinate More Successful. Environ. Health Perspect. 113, 832–835.
- Chi, Z., Xie, Y., Elloy, F., Zheng, Y., Hu, Y., Chen, S., 2013. Bicarbonate-based Integrated Carbon Capture and Algae Production System with alkalihalophilic cyanobacterium. Bioresour. Technol. 133, 513–521. https://doi.org/10.1016/j.biortech.2013.01.150.
- Chi, Z., Elloy, F., Xie, Y., Hu, Y., Chen, S., 2014. Selection of microalgae and cyanobacteria strains for bicarbonate-based integrated carbon capture and algae production system. Appl. Biochem. Biotechnol. 172, 447–457. https://doi.org/ 10.1007/s12010-013-0515-5.
- Cumino, A.C., Perez-Cenci, M., Giarrocco, L.E., Salerno, G.L., 2010. The proteins involved in sucrose synthesis in the marine cyanobacterium Synechococcus sp. PCC 7002 are encoded by two genes transcribed from a gene cluster. FEBS Letters 584 (22), 4655–4660. https://doi.org/10.1016/j.febslet.2010.10.040.
- Davies, F.K., Fricker, A.D., Robins, M.M., Dempster, T.A., McGowen, J., Charania, M., Beliaev, A.S., Lindemann, S.R., Posewitz, M.C., 2021. Microbiota associated with the large-scale outdoor cultivation of the cyanobacterium Synechococcus sp. PCC 7002. Algal Res. 58, 102382 https://doi.org/10.1016/j.algal.2021.102382.
- De Farias Silva, C.E., Sforza, E., Bertucco, A., 2017. Effects of pH and Carbon Source on Synechococcus PCC 7002 Cultivation: Biomass and Carbohydrate Production with Different Strategies for pH Control. Appl. Biochem. Biotechnol. 181, 682–698. https://doi.org/10.1007/s12010-016-2241-2.
- Dokulil, M.T., 2022. Phytoplankton Productivity. In: Mehner, T., Tockner, K. (Eds.), Encyclopedia of Inland Waters, Second Edition. Elsevier, Oxford, pp. 139–153.
- Ducat, D.C., Avelar-Rivas, J.A., Way, J.C., Silvera, P.A., 2012. Rerouting carbon flux to enhance photosynthetic productivity. Appl. Environ. Microbiol. 78 (2012), 2660–2668. https://doi.org/10.1128/AEM.07901-11.
- Durall, C., Lindberg, P., Yu, J., Lindblad, P., 2020. Increased ethylene production by overexpressing phosphoenolpyruvate carboxylase in the cyanobacterium Synechocystis PCC 6803. Biotechnol. Biofuels 13, 1–13. https://doi.org/10.1186/ s13068-020-1653-y.
- Faraloni, C., Torzillo, G., 2017. Synthesis of Antioxidant Carotenoids in Microalgae in Response to Physiological Stress. In: Cvetkovic, D.J., Nikolic, G.S. (Eds.), Carotenoids. InTech.
- Forchhammer, K., Selim, K.A., 2019. Carbon/nitrogen homeostasis control in cyanobacteria. FEMS Microbiol. Rev. 44, 33–53. https://doi.org/10.1093/femsre/fuz025.
- Ghanta, M., Fahey, D., Subramaniam, B., 2014. Environmental impacts of ethylene production from diverse feedstocks and energy sources. Appl. Petrochemical Res. 4, 167–179. https://doi.org/10.1007/s13203-013-0029-7.
- Hajinajaf, N., Fallahi, A., Rabbani, Y., Tavakoli, O., Sarrafzadeh, M.H., 2022. Integrated CO2 Capture and Nutrient Removal by Microalgae Chlorella vulgaris and Optimization Using Neural Network and Support Vector Regression. Waste and Biomass Valorization. https://doi.org/10.1007/s12649-022-01800-2.
- Ji, X., Verspagen, J.M.H., van de Waal, D.B., Rost, B., Huisman, J., 2020. Phenotypic plasticity of carbon fixation stimulates cyanobacterial blooms at elevated CO2. Sci. Adv. 6, 1–10. https://doi.org/10.1126/sciadv.aax2926.
- Kirst, H., Formighieri, C., Melis, A., 2014. Maximizing photosynthetic efficiency and culture productivity in cyanobacteria upon minimizing the phycobilisome lightharvesting antenna size. Biochim. Biophys. Acta - Bioenerg. 1837, 1653–1664. https://doi.org/10.1016/j.bbabio.2014.07.009.
- Knoot, C.J., Ungerer, J., Wangikar, P.P., Pakrasi, H.B., 2018. Cyanobacteria: Promising biocatalysts for sustainable chemical production. J. Biol. Chem. 293, 5044–5052. https://doi.org/10.1074/jbc.R117.815886.
- Latifi, A., Ruiz, M., Zhang, C.C., 2009. Oxidative stress in cyanobacteria. FEMS Microbiol. Rev. 33, 258–278. https://doi.org/10.1111/j.1574-6976.2008.00134.x.
- Ludwig, M., Bryant, D.A., 2012. Synechococcus sp. Strain PCC 7002 transcriptome: Acclimation to temperature, salinity, oxidative stress, and mixotrophic growth conditions. Front. Microbiol. 3, 1–14. https://doi.org/10.3389/fmicb.2012.00354.
- Mangan, N.M., Flamholz, A., Hood, R.D., Milo, R., Savage, D.F., 2016. PH determines the energetic efficiency of the cyanobacterial CO2 concentrating mechanism. Proc. Natl. Acad. Sci. U. S. A. 113, E5354–E5362. https://doi.org/10.1073/pnas.1525145113.

- Melis, A., 2009. Solar energy conversion efficiencies in photosynthesis: Minimizing the chlorophyll antennae to maximize efficiency. In *Plant Science* (Vol. 177 (4), 272–280. https://doi.org/10.1016/j.plantsci.2009.06.005.
- Mullineaux, C.W., Emlyn-Jones, D., 2005. State transitions: An example of acclimation to low-light stress. J. Exp. Bot. 56, 389–393. https://doi.org/10.1093/jxb/eri064.
- Muro-Pastor, M.I., Reyes, J.C., Florencio, F.J., 2005. Ammonium assimilation in cyanobacteria. Photosynth. Res. 83, 135–150. https://doi.org/10.1007/s11120-004-2082.7
- Pathak, J., Rajneesh, Maurya, P.K., Singh, S.P., Häder, D.-P., Sinha, R.P., 2018.
  Cyanobacterial farming for environment friendly sustainable agriculture practices:
  Innovations and perspectives. Front. Environ. Sci. 6 https://doi.org/10.3389/fenvs.2018.00007
- Pniewski, F., 2020. HPLC separation of cyanobacterial and algal photosynthetic pigments. Biologia (Bratisl). 75, 223–233. https://doi.org/10.2478/s11756-019-00407 8
- Qamar, A., Mysore, K.S., Senthil-Kumar, M., 2015. Role of proline and pyrroline-5carboxylate metabolism in plant defense against invading pathogens. Front. Plant Sci. 6, 1–9. https://doi.org/10.3389/fpls.2015.00503.
- Qian, X., Kim, M.K., Kumaraswamy, G.K., Agarwal, A., Lun, D.S., Dismukes, G.C., 2017. Flux balance analysis of photoautotrophic metabolism: Uncovering new biological details of subsystems involved in cyanobacterial photosynthesis. BBA -Bioenerg 1858 (4) 276–387
- Sarnaik, A., Pandit, R., Lali, A., 2017. Growth engineering of Synechococcus elongatus PCC 7942 for mixotrophy under natural light conditions for improved feedstock production. Biotechnology Progress 33 (5), 1182–1192.
- Sarnaik, A., Nambissan, V., Pandit, R., Lali, A., 2018. Recombinant Synechococcus elongatus PCC 7942 for improved zeaxanthin production under natural light conditions. Algal Res. 36, 139–151. https://doi.org/10.1016/j.algal.2018.10.021.
- Sarnaik, A., Abernathy, M.H., Han, X., Ouyang, Y., Xia, K., Chen, Y., Cress, B., Zhang, F., Lali, A., Pandit, R., Linhardt, R.J., Tang, Y.J., Koffas, M.A.G., 2019a. Metabolic engineering of cyanobacteria for photoautotrophic production of heparosan, a pharmaceutical precursor of heparin. Algal Res. 37, 57–63. https://doi.org/10.1016/j.algal.2018.11.010.
- Sarnaik, A., Sawant, K., Khadilkar, J., Pillai, G., Pandit, R., Lali, A., 2019b. Cyanobacterial Cell Factories for Improved Carotenoid Biosynthesis through a Synthetic Biology Approach. ACS Symposium Series. https://doi.org/10.1021/bk-2019-1329.ch002.
- Sawant, K.R., Savvashe, P., Pal, D., Sarnaik, A., Lali, A., Pandit, R., 2021. Progressive transitional studies of engineered Synechococcus from laboratory to outdoor pilotscale cultivation for production of ethylene. Bioresour. Technol. 341, 125852 https://doi.org/10.1016/j.biortech.2021.125852.
- Schellenberger, J., Que, R., Fleming, R.M.T., Thiele, I., Orth, J.D., Feist, A.M., Zielinski, D.C., Bordbar, A., Lewis, N.E., Rahmanian, S., Kang, J., Hyduke, D.R., Palsson, B.Ø., 2011. Quantitative prediction of cellular metabolism with constraint-based models: the COBRA Toolbox v2.0. Quantitative prediction of cellular metabolism with constraint-based models: the COBRA Toolbox 6 (9), 1290–1307.
- Shevela, D., Do, H.N., Fantuzzi, A., Rutherford, A.W., Messinger, J., 2020. Bicarbonate-Mediated CO2Formation on Both Sides of Photosystem II. Biochemistry 59, 2442–2449. https://doi.org/10.1021/acs.biochem.0c00208.
- Singh, A.K., Bhattacharyya-Pakrasi, M., Elvitigala, T., Ghosh, B., Aurora, R., Pakrasi, H. B., 2009. A systems-level analysis of the effects of light quality on the metabolism of a cyanobacterium. Plant Physiol. 151, 1596–1608. https://doi.org/10.1104/pp.109.144824.
- Wang, S., Pan, X., Zhang, D., 2015. PSI Showed Higher Tolerance to Sb(V) than PSII Due to Stimulation of Cyclic Electron Flow Around PSI. Curr. Microbiol. 70, 27–34. https://doi.org/10.1007/s00284-014-0678-5.
- Xiong, W., Morgan, J.A., Ungerer, J., Wang, B., Maness, P.C., Yu, J., 2015. The plasticity of cyanobacterial metabolism supports direct CO2 conversion to ethylene. Nat. Plants 1, 1–6. https://doi.org/10.1038/NPLANTS.2015.53.
- Zhang, Q.W., Lin, L.G., Ye, W.C., 2018. Techniques for extraction and isolation of natural products: A comprehensive review. Chinese Med. (United Kingdom) 13, 1–26. https://doi.org/10.1186/s13020-018-0177-x.
- Zhang, R.L., Wang, J.H., Cheng, L.Y., Tang, Y.J., Chi, Z.Y., 2019. Selection of microalgae strains for bicarbonate-based integrated carbon capture and algal production system to produce lipid. Int. J. Green Energy 16, 825–833. https://doi.org/10.1080/ 15435075.2019.1641103.
- Zhu, C., Chen, S., Ji, Y., Schwaneberg, U., Chi, Z., 2021. Progress toward a bicarbonate-based microalgae production system. Trends Biotechnol. 1–14 https://doi.org/10.1016/j.tibtech.2021.06.005.
- Zhu, T., Xie, X., Li, Z., Tan, X., Lu, X., 2015. Enhancing photosynthetic production of ethylene in genetically engineered Synechocystis sp. PCC 6803. Green Chem. 17, 421–434. https://doi.org/10.1039/c4gc01730g.
- Zhu, C., Zhai, X., Xi, Y., Wang, J., Kong, F., Zhao, Y., Chi, Z., 2020. Efficient CO2capture from the air for high microalgal biomass production by a bicarbonate Pool. J. CO2 Util. 37, 320–327. https://doi.org/10.1016/j.jcou.2019.12.023.
- Zilliges, Y., Lehmann, R., Hoffmann, S., Knoop, H., Gru, M., Lockau, W., Steuer, R., 2013. Flux Balance Analysis of Cyanobacterial Metabolism: The Metabolic Network of Synechocystis sp. PCC 6803, 9. https://doi.org/10.1371/journal.pcbi.1003081.